

Residual Frequency Offset Correction for Coherently Modulated OFDM Systems in Wireless Communication

V.S. Abhayawardhana, I.J. Wassell
Laboratory for Communications Engineering,
Department of Engineering, University of Cambridge, UK
{vsa23,ijw24}@eng.cam.ac.uk

Abstract—Orthogonal Frequency Division Multiplex (OFDM) systems are very sensitive to frequency offset caused by tuning oscillator instabilities and Doppler shifts induced by the channel. The Schmidl and Cox Algorithm (SCA) is quite robust in estimating the frequency offset for systems with large OFDM symbol lengths. It uses two OFDM symbols for training with the first one having two identical halves. The frequency offset is estimated by correlating a received sequence of samples equal to half the OFDM symbol length with the following received samples. The effect of Additive White Gaussian Noise (AWGN) in the estimation process is mitigated only if the number of samples used in the correlation, and hence the OFDM symbol size is large. However to be successfully applied to Broadband Fixed Wireless Access (BFWA) systems, OFDM should perform well even with smaller symbol lengths. In this paper we present the Residual Frequency Offset Correction Algorithm (RFOCA), which uses the SCA for initial frequency offset acquisition and follows it with a stage which reduces the initial residual frequency offset by tracking the phase of the decoded data. We show through simulation that the RFOCA achieves an error variance that is many orders of magnitude lower than at the end of the acquisition stage using the SCA alone.

I. INTRODUCTION

Various solutions have been suggested as contenders to overcome the challenge of transmitting data to the subscriber at high data rates demanded by future broadband applications, for example Broadband Fixed Wireless Access (BFWA), Digital Subscriber Lines (DSL), Cable Modems and Satellite Communication. This paper will address BFWA, owing to its advantages of ease of deployment and cost. Orthogonal Frequency Division Multiplex (OFDM) has been the most popular physical layer standard for BFWA systems due to its robustness and efficiency mainly because it uses a simple Fast Fourier Transform (FFT) of finite length N for modulation and demodulation. Among the standards that have placed their confidence in OFDM are HIPERLAN-2 [1] and IEEE 802.11-a [2].

The orthogonality of the consecutive OFDM symbols is maintained by appending a length v cyclic prefix (CP) at the start of each symbol [3]. The CP is obtained by taking the last v samples of each symbol and consequently the total length of the transmitted OFDM symbols is $(N + v)$ samples. For each OFDM symbol to be independent and to avoid any Inter Symbol Interference (ISI) or Inter Carrier Interference (ICI), the length of the Channel Impulse response (CIR) should be less than $v + 1$ samples. Hence the distortion caused by the CIR only affects the samples within the CP. The receiver discards the CP and takes only the last N samples of each OFDM symbol for demodulation by the receiver FFT. In such a case, the linear convolution of the transmitted signal with the CIR is converted into a circular one. Consequently, for coherently modulated OFDM systems the effects of the CIR can then be equalized by an array of one-tap Frequency Domain Equalizers (FEQ) following the FFT. This is because the frequency selective fading channel can be approximated by a sum of flat fading channels, provided the number of subchannels is large enough. Some-

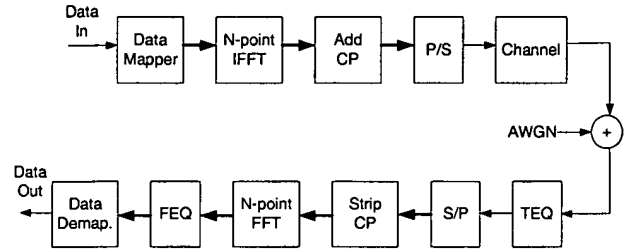


Fig. 1. Block Diagram of the OFDM System

times a Time Domain Equalizer (TEQ) may be used to shorten the effect of the CIR [4]. Figure 1 shows the block diagram of the system, where P/S and S/P represent the Parallel to Serial and Serial to Parallel functions respectively.

Unfortunately, OFDM has been proven to be very sensitive to frequency offset and phase noise caused by tuning oscillator inaccuracies or Doppler shifts induced by the channel. The usual deployment scenario for a BFWA system employs a point to multipoint configuration. Here, a single base station (BS) transmits data in short bursts to many subscriber units (SUs) placed at the user locations. The economic feasibility of a BFWA deployment depends heavily on the cost of the SUs. The use of low cost components, particularly the oscillators, is a major issue since their accuracy and stability are directly related to cost. Hence it is imperative that if OFDM is to be used for BFWA transmission, it should be able to operate effectively using oscillators with only moderate performance and cost.

An OFDM system effectively consists of N sinusoidal subcarriers with frequency spacing $1/T$, where T is the active symbol period of each subcarrier. The k th subcarrier will thus be at $f_k = f_0 + k/T$, where f_0 is a reference frequency. Without loss of generality, we can assume $f_0 = 0$. The modulated subcarriers overlap spectrally, but since they are orthogonal over a symbol duration, they can be easily recovered as long as the channel does not destroy the orthogonality. An unwindowed OFDM system has rectangular symbol shapes. Hence, in the frequency domain the individual subchannels will have the form of sinc functions where the first sidelobe is only some 13 dB below the main lobe of the subcarrier. In the event of a frequency offset between the transmitter and the receiver the subchannels will not align. The effect of frequency offset is two fold, it will reduce the signal power of the desired subchannel outputs and also introduce ICI further increasing the interference levels. The ICI power can be significant even for small frequency offsets in OFDM due to the high sidelobe power of the subchannels. Thus the reduction of frequency offset is critical in OFDM systems. This paper is organised as follows,

section II analyses the effect of frequency offset in OFDM analytically. Section III briefly introduces the Schmidl and Cox Algorithm (SCA) [5] and section IV introduces the novel Residual Frequency Offset Correction Algorithm (RFOCA) that compliments the SCA and improves the performance. Section V shows results obtained by computer simulation and section VI concludes and proposes future work.

II. EFFECT OF FREQUENCY OFFSET IN OFDM

All analysis and simulations in this paper are performed in the digital complex baseband domain. The n th sample of the m th OFDM symbol generated by the Inverse FFT (IFFT) at the transmitter is

$$s_{m,n} = \sqrt{\frac{1}{N}} \sum_{k=0}^{N-1} A_{m,k} e^{j2\pi \frac{kn}{N}}, 0 \leq n \leq N-1 \quad (1)$$

$A_{m,k}$ is the data symbol modulated on to the k th subcarrier of the m th OFDM symbol. The data is converted into a serial sequence, then the CP of length v is added. Thus the m th transmitted OFDM symbol is $\underline{s}(m) = [s_{m,N-v}, \dots, s_{m,N-1}, s_{m,0}, \dots, s_{m,N-1}]^T$. The receiver discards the samples of the CP and uses the samples of the active OFDM symbol for decoding. We assume a finite length CIR with N_h samples, $\underline{h} = [h_0, \dots, h_{N_h-1}]^T$, where $v \geq N_h - 1$. We assume that N is large enough such that the frequency selective channel is divided into contiguous flat fading subchannels. If we assume that correct frame and timing synchronisation is achieved, then the received sequence after stripping the CP can be expressed as,

$$r_{m,n} = \sqrt{\frac{1}{N}} \left\{ \sum_{k=0}^{N-1} A_{m,k} H_k e^{j2\pi \frac{n(k+\epsilon)}{N}} \right\} + w_n \quad (2)$$

for $0 \leq n \leq N-1$. Here H_k is the transfer function of the channel at the subchannel index k , w_n is the Additive White Gaussian Noise (AWGN) term and ϵ is the frequency offset relative to the intercarrier spacing. The symbol after FFT demodulation is

$$Y_{m,l} = \sqrt{\frac{1}{N}} \sum_{n=0}^{N-1} r_{m,n} e^{-j2\pi \frac{ln}{N}}, 0 \leq l \leq N-1 \quad (3)$$

Substituting (2) into (3) allows the output of the l th subchannel to be expressed as the sum of three components.

$$Y_{m,l} = (A_{m,l} H_l) \frac{\sin(\pi\epsilon)}{N \sin(\pi\epsilon/N)} e^{j\pi\epsilon \frac{N-1}{N}} + I_l + W_l \quad (4)$$

The first term on rhs of equation 4, denoted R_l hereafter, shows that the desired term $A_{m,l} H_l$ experiences amplitude reduction and phase distortion. As $N \gg \pi\epsilon$, $N \sin(\pi\epsilon/N)$ can be approximated by $\pi\epsilon$. Hence the degradation of the required term vanishes when the received data does not experience any frequency offset. In practice, the effect of the channel transfer function H_l is removed by the FEQ following the FFT. Note that the FEQ is trained by transmitting a known training symbol occupying the OFDM symbol number N_t , $\underline{\hat{A}} = [A_{N_t,0}, \dots, A_{N_t,N-1}]^T$. Usually the training symbol is placed at the beginning of the frame. The ratio of the

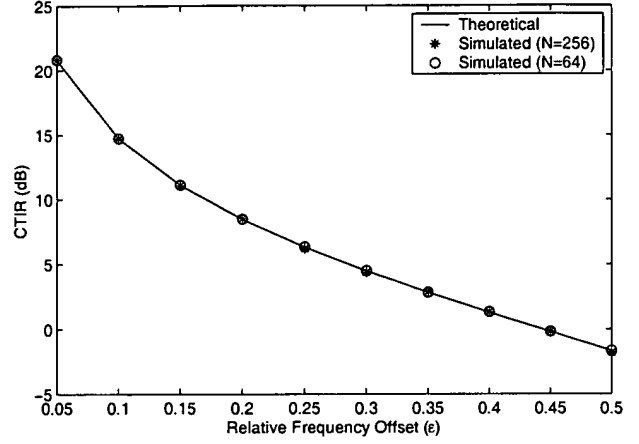


Fig. 2. Analysis of CTIR vs Relative Frequency Offset, ϵ

decoded samples of the training symbol $Y_{N_t,l}$, to the locally generated copy of $A_{N_t,l}$, where $0 \leq l \leq N-1$, is used to calculate the coefficients for the FEQ.

The second term in equation (4) is the ICI and the third term is due to the AWGN. The ICI term is given as,

$$I_l = \sum_{\substack{k=0 \\ k \neq l}}^{N-1} (A_{m,k} H_k) \frac{\sin \pi(k + \epsilon - l)}{N \sin \pi(k + \epsilon - l)/N} e^{j\pi(k + \epsilon - l) \frac{N-1}{N}} \quad (5)$$

If we assume that the transmitted data is zero mean and uncorrelated (i.e. $E[A_{m,k}] = 0$ and $E[A_{m,l} A_{m,k}^*] = |A|^2 \delta_{l,k}$), then $E[I_l] = 0$. Hence the ICI power is,

$$E[|I_l|^2] = |A|^2 [\sin \pi\epsilon]^2 \sum_{\substack{k=0 \\ k \neq l}}^{N-1} \frac{E[|H_k|^2]}{[N \sin \pi(k + \epsilon - l)/N]^2} \quad (6)$$

To appreciate the severity of frequency offset on the Carrier to Interference Ratio (CTIR) in an OFDM system, we define $CTIR = E[|R_l|^2]/E[|I_l|^2]$. Assuming the channel transfer function, H is unity and with zero AWGN, (i.e. $W_l = 0$), then

$$CTIR = \frac{\sum_{\substack{k=0 \\ k \neq l}}^{N-1} 1/[N \sin \pi(k + \epsilon - l)/N]^2}{[N \sin(\pi\epsilon/N)]^2} \quad (7)$$

A similar analysis on the effect of frequency offset on OFDM can be found in [6] and [7]. Figure 2 shows CTIR in decibels as a function of ϵ . Simulated values for $N = 64$ and 256 using QPSK data mapping are also shown. It shows that the CTIR drops significantly when relative frequency offset, ϵ increases beyond 0.1. An important observation is that the CTIR is independent of N .

III. SCHMIDL AND COX ALGORITHM (SCA)

One of the more robust schemes to estimate both frame synchronisation and frequency offset is the SCA. It uses two training symbols with the first one having a repetition within half a symbol period. Frame synchronisation is achieved by searching for a training symbol with two identical halves. If $L = N/2$, the sum

of L consecutive correlations between pairs of samples spaced L apart is found as,

$$P(d) = \sum_{n=0}^{L-1} (r_{d+n}^* r_{d+n+L}) \quad (8)$$

The output of the correlator, as given by (8) will reach a peak at the end of the CP of the first training symbol. If $v > N_h - 1$ and $p = v - (N_h - 1)$, the peak is actually maintained for p samples just before the end of the CP of the first training symbol. Thus the correlator output will take the form of a plateau. This is because the last few samples of the CP, equal to the length of p , are not corrupted by the CIR. Timing synchronisation is achieved by locating the end of this plateau, denoted by d_{opt} . Since the CP ensures that there is no Inter Block Interference (IBI) between OFDM symbols, the effect of the CIR in the first training symbol is cancelled if the conjugate of a sample from the first half is multiplied by the corresponding sample from the second half. Hence the phase difference between the two halves of the first training symbol is caused by the frequency offset, $\phi = \pi\epsilon$. It can be estimated as $\hat{\phi} = 1/p \sum_{n=0}^p \angle P(d_{opt} - n)$. If $\epsilon < 1$ there is no phase ambiguity in $\hat{\phi}$ and the frequency offset can be estimated as

$$\hat{\epsilon}_{SCA} = \hat{\phi}/\pi \quad (9)$$

In order to resolve potential ambiguity use can be made of the second training symbol, as detailed in [5]. The effect of AWGN on the partial estimation given by equation (9) is insignificant only if L , and hence the number of FFT points N , is large. The SCA performs well for OFDM systems with N in excess of 1000 [5]. For BFWA systems, data is transmitted in short bursts, particularly in the uplink. In this situation, it would be wasteful to use an OFDM system with large N . Besides large values of N will give rise to the additional problems of high peak-to-average power ratio and will also introduce latency which reduces protocol efficiency. Typically BFWA systems utilise lower values of N such as 64 to 256 as presented in [1] and [2]. When the SCA is used for systems with lower values of N , the estimate $\hat{\epsilon}$ is not sufficiently accurate. This error results in a residual frequency offset that rotates the received constellation at a reduced rate, but one that is still significant enough to cause bit errors in coherently demodulated OFDM systems. In this paper we present the Residual Frequency Offset Correction Algorithm (RFOCA) that compliments the SCA by following it with a tracking function that continuously compensates for the residual frequency offset error.

Other approaches that are used for frequency offset correction include for example the use of null symbols [8]. The use of a null symbol is not practical in a burst mode system as the transmission will always be a null while no data is transmitted. Other suggestions utilise the correlation between the cyclic prefix and the last few samples of the OFDM symbol [9] and the self-cancellation schemes presented in [10] and [7], where the same data is sent in more than one subchannel. Both schemes are not very practical when N is a low value with the latter two approaches having the additional problem of reducing the number of useful subchannels by at least half. Note that the RFOCA does not utilise any pilots nor null symbols yet will be shown to effectively eliminate the residual offset. The proposal in [11] also attempts to track the

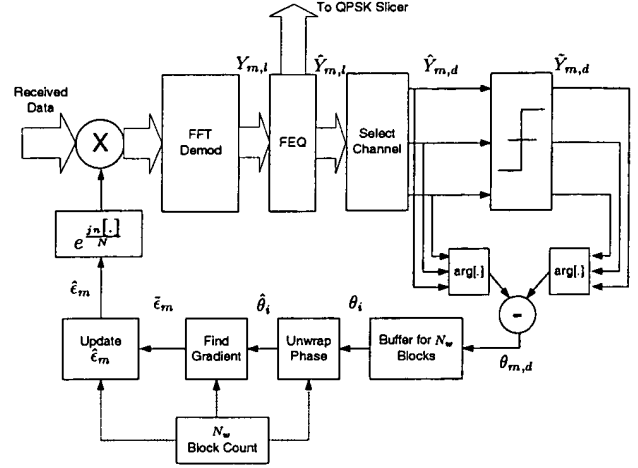


Fig. 3. Residual Frequency Offset Correction Algorithm (RFOCA)

residual frequency offset. Here, the residual offset correction factor is updated at the end of each OFDM symbol. However our tests indicate that the estimate is not very accurate when only one symbol is used, hence we update the residual offset correction factor only after analysing a block of N_w , ($N_w > 1$) OFDM symbols.

IV. RESIDUAL FREQUENCY OFFSET CORRECTION ALGORITHM (RFOCA)

In the proposed approach, an initial frequency offset acquisition is made using the SCA. We propose to estimate the residual frequency offset, $\tilde{\epsilon}$ by tracking the rate of phase change at the FEQ outputs, $\hat{Y}_{m,l}$ as shown in Figure 3. However, the estimate of $\tilde{\epsilon}$ could be seriously affected by subchannels with a low SNR resulting from spectral nulls in the channel response H_l . An estimate of H_l is made by taking the ratio of the transmitted and decoded output of the second training symbol of the SCA. Hence we only select those subchannels with $|H_l|$ above a certain threshold. We call this subset of subchannels $\underline{d} \subset [0, \dots, N-1]$. The criteria applied is to select subchannels with $|H_l|$ in excess of a standard deviation above the mean. For symbol m , the outputs of these subchannels $\hat{Y}_{m,d}$ are sent through a slicer to obtain $\tilde{Y}_{m,d}$, where $d \in \underline{d}$.

For symbol m the phase errors between $\hat{Y}_{m,d}$ and $\tilde{Y}_{m,d}$, namely $\theta_{m,d}$ are found as,

$$\theta_{m,d} = \angle \hat{Y}_{m,d} - \angle \tilde{Y}_{m,d} \quad (10)$$

The phase errors are stored in a buffer, \underline{b} for a block of N_w OFDM symbols. Note that only the selected subchannels will be stored. Hence if the number of subchannels selected in \underline{d} is N_d then the length required for the buffer is only $N_d N_w$. The Maximum Likelihood (ML) estimate of the residual frequency offset $\tilde{\epsilon}$ is calculated as the gradient of the values stored in the buffer. Note, in this paper we have assumed QPSK data mapping though the technique could be extended to other constellations. Initially, $\tilde{\epsilon}$ can be quite high and if the values of the phase errors, $\theta_{m,d} > \pi/4$, then it results in decoding errors being produced by the slicer which subsequently results in phase wrapping of $\theta_{m,d}$ at $\pm\pi/4$. Hence it is imperative that we first unwrap $\theta_{m,d}$ before the calculation of

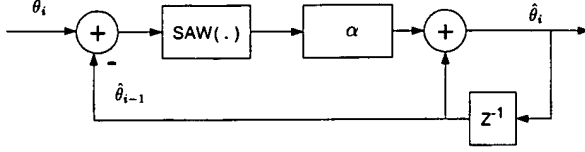


Fig.4. Phase Unwrapping Algorithm

$\tilde{\epsilon}$. Although accurate phase unwrapping algorithms are available, they are very complex. Since we are only interested in the phase gradient and not the exact phase values, a simpler scheme was selected for the unwrapping of the phase [12]. For purposes of clarity, we denote the i th sample of the wrapped phase and the unwrapped phase as θ_i and $\hat{\theta}_i$, respectively. The phase unwrapping algorithm can be expressed as

$$\hat{\theta}_i = \hat{\theta}_{i-1} + \alpha \text{SAW}(\theta_i - \hat{\theta}_{i-1}) \quad (11)$$

where $\text{SAW}(\cdot)$ is a sawtooth function that limits the output to $\pm\pi/4$ and α is a parameter that controls the variance of the unwrapped phase. The algorithm is illustrated in Figure 4.

The error due to frequency offset is compensated by multiplying the pre-FFT received symbols, $r_{m,n}$ with $e^{jn\hat{\epsilon}_m/N}$, where in general $\hat{\epsilon}_m$ is the frequency offset correction factor for symbol m , which is initialised to $\hat{\epsilon}_{SCA}$ at the acquisition stage. At symbol number qN_w , $\hat{\epsilon}_{qN_w}$ is updated according to $\hat{\epsilon}_{qN_w} = \hat{\epsilon}_{qN_w-1} + \tilde{\epsilon}_{qN_w}$, where q is a positive integer. For OFDM symbols $[(q-1)N_w, qN_w-1]$, $\hat{\epsilon}_{(q-1)N_w}$ is used as the frequency offset correction factor. In other words $\hat{\epsilon}_m$ is updated once every N_w OFDM symbol blocks.

The choice of N_w is critical as a large value will cause the updating of $\hat{\epsilon}_m$ with too high a latency. However after a few updates the values of $\tilde{\epsilon}$ are quite small, hence to get a better estimate in the presence of AWGN a larger value of N_w will reduce the variance. The RFOCA can be summarised as follows.

1. Do an initial frequency offset acquisition $\hat{\epsilon}_{SCA}$ using the SCA.
2. Select the subset of subchannels with magnitudes exceeding the defined threshold in the channel transfer function, \underline{d} , at the start of the burst.
3. Obtain $\hat{Y}_{m,d}$ from the FEQ output and then $\tilde{Y}_{m,d}$ by use of a slicer for each symbol m , where $d \in \underline{d}$. Calculate and store $\theta_{m,d}$ for a block of N_w OFDM symbols.
4. Find the unwrapped phase $\hat{\theta}$ from the wrapped phase θ . Find the gradient of $\hat{\theta}$, namely $\tilde{\epsilon}$. This process is done once every N_w symbols.
5. Once every N_w OFDM symbol block, calculate the new frequency offset correction factor $\hat{\epsilon}_{qN_w}$.

V. SIMULATION PARAMETERS AND RESULTS

OFDM systems with $N = 64, 128, 256$ have been simulated at a sampling rate of 20 MHz with a guard interval equal to 20 samples, thus the subcarrier spacings are approximately 312 kHz, 156 kHz and 78 kHz respectively. QPSK mapping for all subchannels has been employed and all the subchannels are used. A burst of 320000 data bits is assumed to be transmitted. Each data point in the simulation results is obtained by averaging over 500 such bursts. In order to test the performance of the RFOCA with frequency offset alone, we have assumed perfect symbol and frame

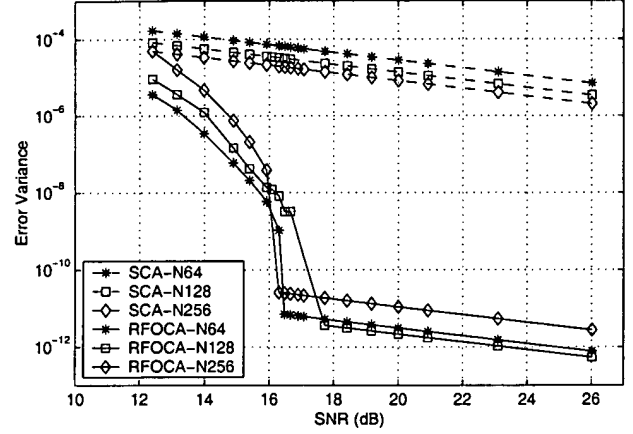


Fig. 5. Comparison of Error Variances of SCA and RFOCA in AWGN for $N = 64, 128, 256$ and $\epsilon = 0.5$

synchronisation for the simulated coherent OFDM systems. A more robust symbol synchronisation algorithm that virtually guarantees perfect frame synchronisation will be the subject of a future publication. After much testing, the values selected for N_w were 250, 250, 125 for $N = 64, 128, 256$, respectively. Figure 5 shows the comparison of error variances at the end of the acquisition stage using the SCA and the tracking stage using the RFOCA for $N = 64, 128, 256$ as a function of the Signal to Noise Ratio (SNR), with $\epsilon = 0.5$. It shows that the RFOCA error variance is many orders of magnitude lower than at the end of the acquisition stage. There appears to be a threshold effect in RFOCA at around an SNR of 16 dB, below which the error variance increases rapidly. It is mainly due to the errors present in the selected subchannels of \underline{d} , which subsequently create estimation errors in the residual offset, $\tilde{\epsilon}_m$. Figure 6 shows the performance of the RFOCA in terms of Bit Error Rate (BER) vs SNR again in AWGN. The BER is virtually zero at values of SNR above 16 dB but suddenly increases below 16 dB. This result is a direct consequence of the threshold effect observed with the previous error variance results. It is observed that at an SNR of 16 dB only a few out of the total of 500 received bursts give rise to errors. However, these errors are significant giving rise to a high overall BER. Such occurrences became more common when the SNR is reduced below 15 dB, thus increasing the BER very rapidly.

Appropriate models for BFWA channels are in the process of being defined. The Stanford University Interim (SUI) channels comprise 6 models for 3 different terrain conditions [13]. All of them are simulated using 3 taps, each having either Rayleigh or Ricean amplitude distributions. The channel is assumed to be wide-sense stationary uncorrelated scattering (WSSUS) and each tap of the CIR is modeled as $h_i = \beta_i e^{j\phi_i}$, where the amplitude β_i and the phase ϕ_i are selected independently [14]. The burst takes less than 10 ms to transmit at the selected sampling frequency, consequently the channel is assumed constant for the duration of each burst. We have selected the SUI-2 channel model, pertaining to terrains with low tree densities and with antennas having a directivity of 30 degrees at the SU and 120 degrees at the BS. The channel is characterised by a RMS delay spread of 0.2 μ s.

Figure 7 allows a comparison of the error variances of the SCA

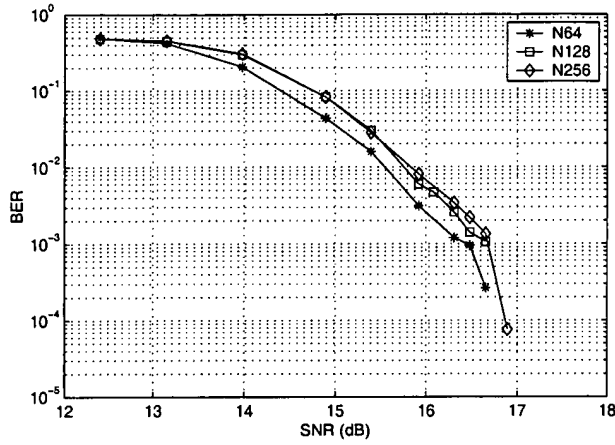


Fig. 6. Performance of RFOCA in AWGN for $N = 64, 128, 256$ and $\epsilon = 0.5$

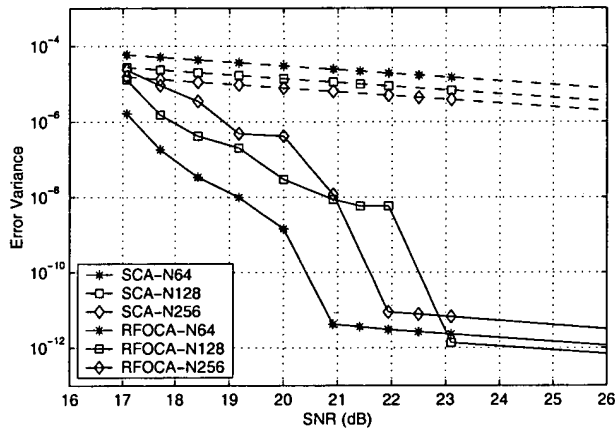


Fig. 7. Comparison of Error Variances of SCA and RFOCA with AWGN and SUI-2 CIR for $N = 64, 128, 256$ and $\epsilon = 0.5$

and the RFOCA for an OFDM system with $\epsilon = 0.5$ in the SUI-2 channel. A new channel in accordance with the SUI-2 profile is randomly generated for the transmission of each burst. The RFOCA error variance is seen to be many orders of magnitude lower than at the end of the acquisition stage despite the presence of the SUI-2 channel.

Figure 8 shows the performance of the RFOCA in terms of BER vs SNR for the SUI-2 channel and $\epsilon = 0.5$. The threshold effect now occurs at an SNR in the region of 20 dB owing to the effect of the SUI-2 channel.

VI. CONCLUSION

We have presented a Residual frequency Offset Correction Algorithm (RFOCA), that compliments the frequency acquisition process performed by the Schmidl and Cox Algorithm (SCA). The RFOCA continuously tracks and compensates for the residual frequency offset that is present after the acquisition stage. We have applied the RFOCA for AWGN and BFWA channels, namely the SUI-2 channel profile, and have shown a significant reduction in the error variance brought about by the use of the RFOCA following the initial acquisition stage. Although the algorithm may appear to suffer from a threshold effect it still gives a significant

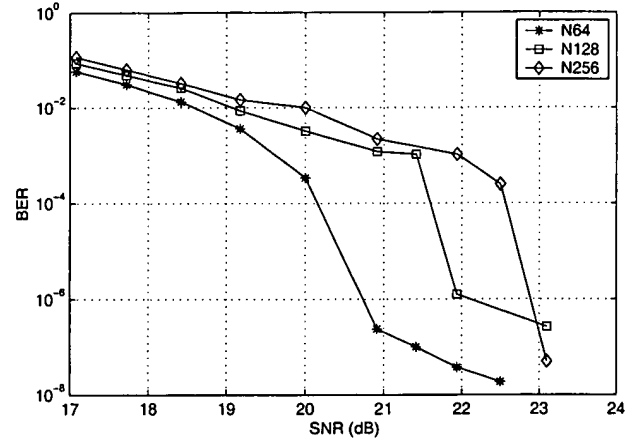


Fig. 8. Performance of RFOCA with AWGN and SUI-2 CIR for $N = 64, 128, 256$ and $\epsilon = 0.5$

performance advantage at realistic signal to noise ratios. In the future we hope to address the threshold effect by improving the phase unwrapping and investigating other criteria for the selection of the subchannels. We also hope to improve the performance of the SCA in a frame synchronisation role.

REFERENCES

- [1] ETSI, *Broadband Radio Access Networks (BRAN); HIPERLAN-2; Physical Layer*, April 2000.
- [2] R. van Nee, G. Awater, M. M. H. Takanashi, M. Wester, and K. Halford, "New high-rate wireless LAN standards," *IEEE Communication Magazine*, vol. 37, pp. 82–88, December 1999.
- [3] A. Peled and A. Ruiz, "Frequency domain data transmission using reduced computationally complexity algorithms," in *Proceedings of IEEE International Conference of Acoustics, Speech and Signal Processing*, (Denver), pp. 964–967, April 1980.
- [4] V. S. Abhayawardhana and I. J. Wassell, "Frequency scaled time domain equalization for OFDM in broadband fixed wireless access channels," in *Proceedings of the IEEE Wireless Communications and Networking Conference*, 2002. to be presented.
- [5] T. M. Schmidl and D. Cox, "Robust frequency and timing synchronisation for OFDM," *IEEE Transactions on Communications*, vol. 45, pp. 1613–1621, December 1997.
- [6] P. H. Moose, "A technique for orthogonal frequency division multiplexing frequency offset correction," *IEEE Transactions in Communications*, vol. 42, pp. 2908–2914, October 1994.
- [7] Y. Zhao and S.-G. Haggman, "Intercarrier interference self-cancellation scheme for OFDM mobile communication systems," *IEEE Transactions on Communications*, vol. 49, pp. 1185–1191, July 2001.
- [8] H. Nogami and T. Nagashima, "A frequency and timing period acquisition technique for OFDM systems," in *Proceedings of Personal, Indoor and Mobile radio Communication (PIMRC)*, pp. 1010–1015, September 1995.
- [9] J.-J. van de Beek and M. Sandell, "ML estimation of time and frequency offset in OFDM systems," *IEEE Transactions on Signal Processing*, vol. 45, pp. 1800–1805, July 1997.
- [10] J. Armstrong, "Analysis of new and existing methods of reducing intercarrier interference due to carrier frequency offset in OFDM," *IEEE Transactions on Communications*, vol. 47, pp. 365–369, March 1999.
- [11] H. Kobayashi, "A novel coherent demodulation for M-QAM OFDM signal operating in the burst mode," in *Proceedings of the IEEE Vehicular Technology Conference (Fall)*, vol. 3, pp. 1387–1391, September 2000.
- [12] H. Meyr, M. Moeneclaey, and S. Fechtel, *Digital Communication Receivers; Synchronization Channel Estimation and Signal Processing*. John Wiley & Sons Inc., 1998.
- [13] V. Erceg, K. Hari, et al., "Channel models for fixed wireless applications," tech. rep., IEEE 802.16 Broadband Wireless Access Working Group, January 2001.
- [14] K. Pahlavan and A. Levesque, *Wireless Information Networks*. New York: J. Wiley & Sons, 1995.